Proceedings of 12th Cambridge Workshop on Cool Stars, Stellar Systems, & The Sun, 2003 University of Colorado.

Spotted Stars in the Pleiades and Orion Nebular Cluster

Th. Granzer[1], K. G. Strassmeier[1]

Abstract. We present the results of extensive MHD simulations aiming to predict star spot patterns on stars in two well-known stellar clusters, the Pleiades (100 Myr) and the Orion Nebular Cluster (2 Myr). The emergence of thin magnetic flux tubes is studied from their origin at the base of the convective zone up to the photosphere. The mass/rotational grid of the stellar models is wide enough to cover all stellar types where theory predicts the possibility of starspot formation. In particular, masses between 4.0 $M_\odot$ and 0.4 $M_\odot$ and rotational rates from 0.25 $\Omega_\odot$ to 25 $\Omega_\odot$ are considered.

1. Cluster Star Models

To successfully apply our thin-flux-tube-evolution code, the underlying stellar model must obey a certain 'layout', i.e., an outer convective envelope is followed by an inner radiative zone. The interface layer is a region suitable for storing and amplifying of magnetic flux: The stratification is subadiabatic, thus suppressing magnetic buoyancy, but overshooting convective elements provide enough helicity to drive a (unspecified) dynamo.

For ages of 100 Myr (Pleiades) and 2 Myr (Orion Nebular Cluster) the stellar models are summarized in Tab. 1. See also Fig. 1 for a theoretical HR-diagram of the two clusters. Only models with a non-vanishing R_c/R_* can be considered.

All stellar models are derived from fully-convective polytropic start-models evolved with the MLT-version of the Kippenhahn et al. code (1967). To reflect improvements in the equation of state (eos) and the opacities, the code has been updated to OPAL eos (Rogers et al., 1996) and opacities (Iglesias & Rogers, 1996), the latter being extended to low temperatures with the Alexander & Ferguson (1994) tables. The properties of the overshoot region were calculated afterwards, following the prescriptions of Shaviv & Salpeter (1973). Rotation has not been taken into account for the calculation of the stellar model, but was introduced later by simply spinning-up the non-rotating stellar models from the stellar-evolution code.

A 4.0 $M_\odot$ star was included in the Pleiades to allow comparison of pre-main-sequence models with a giant star model. Note that the age of this star is *not* 100 Myr as for the other Pleiades stars, but 137 Myr. Aging of the 4.0 $M_\odot$ beyond 100 Myr was necessary to yield the required internal structure. Additionally, tuning the age to 137 Myr allows a direct comparison of this model

[1]Astropysical Institute Potsdam

Orion Nebular, 2 Myr				Pleiades, 100 Myr			
M	$L/\mathrm{L}_\odot$	$T_{\mathrm{eff}}/\mathrm{K}$	R_c/R_*	M	$L/\mathrm{L}_\odot$	$T_{\mathrm{eff}}/\mathrm{K}$	R_c/R_*
0.4	0.304	3840	—	0.4	0.0357	3760	0.393
0.6	0.571	4100	—	0.6	0.0841	4070	0.598
0.8	0.891	4290	—	0.8	0.316	4990	0.673
1.0[1]	1.021	4440	0.260	1.0	0.694	5610	0.726
1.3	1.879	4530	0.325	1.3	2.524	6500	—
1.6	2.837	4880	0.435	1.6	6.480	7550	—
2.0	4.595	5110	0.531	2.0	16.48	9120	—
2.5	9.757	5460	0.661	2.5	40.71	10750	—
4.0	231.4	14780	—	4.0[2]	211.1	4680	0.397

[1] 2.5 Myr old

[2] 137 Myr old

Table 1. Stellar models calculated for flux-tube evolution. Left half of the table refers to models of the Orion Nebular cluster. Right half of the table refers to models of the Pleiades. M is the mass of the star in $\mathrm{M}_\odot$, R_c is the size of the radiative core in fractions of the stellar radius.

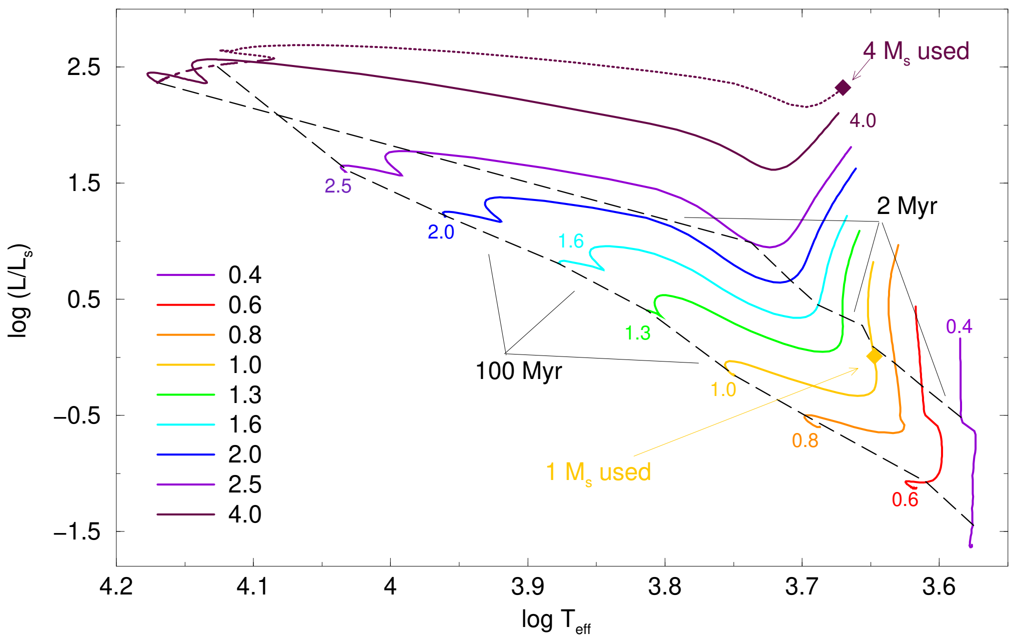

Figure 1. A theoretical HR-diagram of stars in the mass range of 0.4 to 4.0 $\mathrm{M}_\odot$. The isochrones for the age of the Orion Nebular cluster (2 Myr) and the Pleiades (100 Myr) are indicated. The slightly more evolved 1 $\mathrm{M}_\odot$ stellar model of Orion and the 4 $\mathrm{M}_\odot$ stellar model of the Pleiades are indicated with diamonds.

with the Pleiades 0.4 $M_\odot$ model, see the discussion section. For the Orion cluster a 1.0 $M_\odot$ star was included at an age of 2.5 Myr, again due to structural requirements.

2. Flux-Tube Models

We use the well-known *thin-flux-tube approximation* (e.g. Spruit, 1981) to model the ascent of magnetic flux from the overshoot region to the surface. Amongst other drawbacks of this approach is the violation of this approximation in near-surface layers which prohibits any model-based predictions on post-emergence development of the starspots. Velocity fields *below* the surface layers can be taken into account, but for all stars other than our Sun our knowledge is very limited. Thus, all simulations are carried out with a rigid rotational profile. A flux tube in an initial stable *mechanic* equilibrium inside the overshoot region is exposed to a small (undulatory) disturbance which eventually grows and leaps out of the overshoot region into the convective envelope. Here, the superadiabatic stratification amplifies the growth of the disturbance which evolves into a (single) rising loop. The simulation must cease as the thin flux tube approximation breaks down due to the vast drop of the pressure scale height near the surface layers. In all studied cases, the flux tube-summits reach, however, an elevation of approximately 0.98 $R_\star$. The straight extension to the surface of these end-points of the simulation is considered the emergence latitude of a starspot; twelve individual flux tubes with different equilibrium latitudes inside the overshoot layer (5° to 60°) are combined to yield the *spot probability function, SPF*, a normalized measure of probability of starspot formation as a function of latitude, see Figs. 2 and 3 for examples. Colored areas indicate regions of spot formation, the probability rising as the appropriate area widens.

3. Orion Nebular Cluster

The Orion Nebular cluster is one of the youngest clusters known. Various authors derive an age of the cluster of approximately 2 Myr, with a considerable star-formation rate spanning the last 4 million years. To make different masses more comparable, we restricted the evolutionary age of our stellar models to exactly 2 Myr. At this age only masses between 2.5 and 1.0 $M_\odot$ show a radiative core and an outer convective layer.

In Fig. 2, the spot probabilities for five different rotational periods are plotted. Four points are evident.

- For the higher masses, above 1.6 $M_\odot$, an almost linear increase of the spot latitude with rotation rate is seen.
- For these models, the lighter ones generally show higher spot occurrence at a fixed rotational period.
- The spot latitudes in the 1.3 $M_\odot$ model are almost independent of the rotational rate and spot occurrence is generally very restricted to a 10° area around 35° latitude.

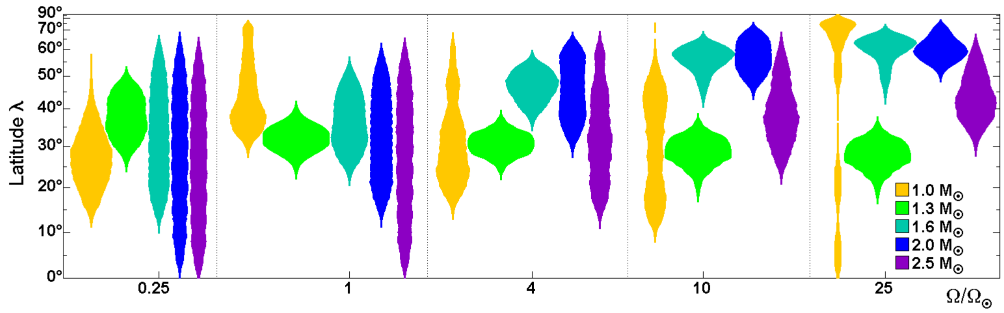

Figure 2. Latitudinal spot probabilities of a 1.0, 1.3, 1.6, 2.0, and 2.5 $M_\odot$ stellar model in the Orion Nebular cluster (color coded). Five different rotational rates, 0.25, 1, 4, 10, and 25 $\Omega_\odot$ are shown.

- The 1.0 $M_\odot$ star at $\Omega = 25\Omega_\odot$ shows activity at all latitudes, with pronounced polar activity.

4. Pleiades

The Pleiades are one of the most studied clusters. Various authors place its age at around 100 Myr. Again, to yield easy-comparable results, we restricted the calculation of the stellar models to exactly 100 Myr. At this age only masses below 1.0 $M_\odot$ show the required structure. Masses up to 4.0 $M_\odot$ are either fully radiative or have an outer radiative zone. Masses even higher than 4.0 $M_\odot$ are already in their giant stages, but hard to reach with our stellar evolution code. To allow at least some principle statements on flux tube evolution in giants, we included a 4.0 $M_\odot$ at an age of 137 Myr in our calculations. The age was somehow arbitrarily fixed, but it was tailored to yield a stellar model whose radiative core is exactly the same fractional size as for the 0.4 $M_\odot$ model. This was especially useful for inter-comparison between the different masses.

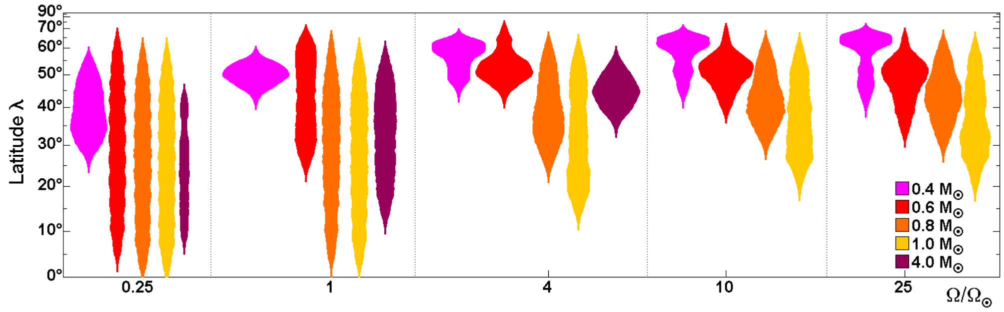

Figure 3. Latitudinal spot probabilities of a 0.4, 0.6, 0.8, 1.0, and 4.0 $M_\odot$ stellar model in the Pleiades cluster (color coded). Five different rotational rates, 0.25, 1, 4, 10, and 25 $\Omega_\odot$ are shown.

In Fig. 3, the spot probabilities for five different rotational periods are plotted. Again, four points are evident.

- For all masses considered, an increase of spot latitude with rotation is seen.
- Again, for a fixed rotational period, the lighter masses show higher spot latitudes, except for the 4.0 $M_\odot$ giant.
- At low rotational periods, no difference between the 1.0 and 0.8 $M_\odot$ model is visible.
- The 4.0 $M_\odot$ shows no flux-tube emergence at rotation rates above 4 $\Omega_\odot$.

5. Discussion

An increase of spot latitude with rotational rate is evidently proved, at least for stars with rather big radiative cores. Looking carefully at the spot probabilities of the individual models and comparing them to the core sizes in Tab. 1, one gets the impression that the relative size of the core is another key ingredient in understanding the star spot patterns. To test this assumption, we plot the spot probabilities of all models at the fixed rotation rate of $\Omega = 4\ \Omega_\odot$ in Fig. 4. On the x-axis the relative core size is plotted.

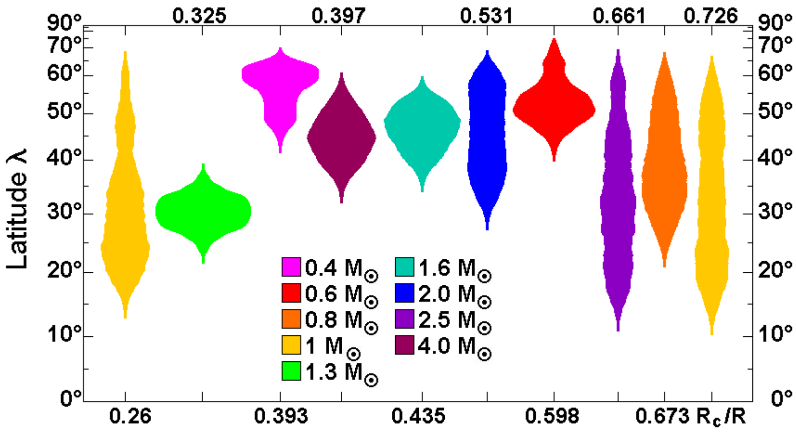

Figure 4. Latitudinal spot probabilities of all stellar models at a fixed rotation rate of $\Omega = 4\ \Omega_\odot$. The x-axis is relative core size.

One sees that the emergence latitude decreases with increasing core size. This can be explained as a geometrical effect: flux tubes rising vertically will reach higher latitudes if they origin closer to the center of the star, i.e. if the core is smaller. Another effect, seen especially in the 0.6 and 0.8 $M_\odot$ model, is the more pronounced pole-ward deflection for less-massive stars.

The magnetic tension may be responsible for the total lack of flux tube emergence in the 4.0 $M_\odot$ star once a rotation rate of $\Omega = 4\ \Omega_\odot$ is passed. In our simulation we see the flux tube starting to emerge but stalling half the way up through the convective layer. Like in a rubber band, the magnetic tension then

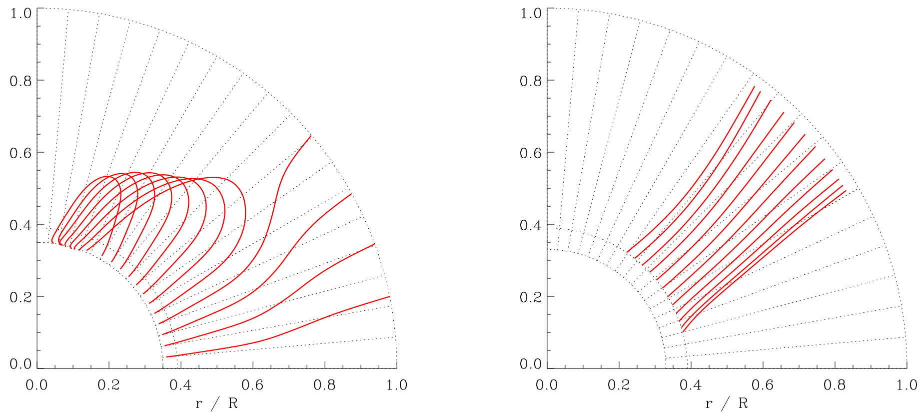

Figure 5. Comparison of the flux-tube summit rise in a 4.0 $M_\odot$ (left) and 0.4 $M_\odot$ Pleiades model (right). Both stars rotate at $\Omega = 0.25\ \Omega_\odot$. Flux-tubes originating from the overshoot layer at latitudes above 20° attain a new equilibrium at high latitudes well inside the overshoot layer.

forces the flux-tube to contract again, at last finding a new stable equilibrium at the base of the convective zone. During the remaining time of the simulation the flux tube remains in this newly attained equilibrium, parallel to the equator at high latitudes around 70° and up. Fig. 5 illustrates this process and makes a direct comparison of the flux-tube rise-pattern in a 0.4 $M_\odot$ with identical rotation rate of $\Omega = 0.25\ \Omega_\odot$.

Another team (Holzwarth & Schüssler, in press) report a similar behaviour for less massive giants. The entire mechanism responsible for forcing the flux tube to the new equilibrium is not fully worked out yet, but further studies may bring more insight. What can be stated, though, is that the emergence patterns in evolved giants will fundamentally differ from the emergence patterns in young and main sequence stars (refer also to Fig. 3). Note that the relative core size of the 0.4 and the 4.0 $M_\odot$ star is almost identical and thus the star spot patterns should be similar, but they are strikingly different.

References

Kippenhahn R., Weigert A., & Hofmeister E., 1967, Meth. Comp. Phy., 7, 129

Rogers F. J., Swenson F. J., & Iglesias C. A., 1996, 1995, ApJ, 456, 902 (OPAL eos)

Iglesias C. A. & Rogers F. J., 1996, ApJ, 464, 943 (OPAL opacities)

Alexander D. R. & Ferguson J. W., 1994, ApJ, 437, 879

Shaviv G. & Salpeter E. E., 1973, ApJ, 184, 191

Spruit H. C., 1981, A&A, 98, 155

Holzwarth V. & Schüssler M., A&A, in press